01 Jan 1993

A Pulsed Power Design for the Linear Inductive Accelerator Modules for the Laboratory Microfusion FA

Ronald E. Olson
Missouri University of Science and Technology, olson@mst.edu

D. L. Smith

M. G. Mazarakis

L. F. Bennett

et. al. For a complete list of authors, see https://scholarsmine.mst.edu/phys_facwork/322

Recommended Citation

R. E. Olson et al., "A Pulsed Power Design for the Linear Inductive Accelerator Modules for the Laboratory Microfusion FA," *Pulsed Power Conference*, Institute of Electrical and Electronics Engineers (IEEE), Jan 1993.
The definitive version is available at https://doi.org/10.1109/PPC.1993.513364

A PULSED POWER DESIGN FOR THE LINEAR INDUCTIVE ACCELERATOR MODULES FOR THE LABORATORY MICROFUSION FACILITY

David L. Smith, Michael G. Mazarakis, Lawrence F. Bennett,
Tom R. Lockner, Richard E. Olson, George O. Allshouse, and John D. Boyes
Sandia National Laboratories
P.O. Box 5800, Albuquerque, NM 87185

Abstract

Upon achieving ignition and gain, the Laboratory licrofusion Facility (LMF) will be a major tool for iertial Confinement Fusion (ICF) research and defense pplications. Our concept for delivering ~10 MJ with a eak on-target light ion power of ~700 TW involves a iulti-modular approach using an extension of the compact iductively isolated cavity and Magnetically Insulated 'ransmission Line (MITL) Voltage Adder technology that presently being used in several large accelerators at andia/New Mexico. The LMF driver design consists of welve 8-TW and twelve 38-TW accelerating modules, each ith a triaxial MITL/Adder[1] that delivers power to a two age ion extraction diode.[2] The desired energy, power ulse shape, and deposition uniformity on an ICF target an be achieved by controlling the energy and firing equence of the "A" and "B" accelerator modules, plus ptimizing the beam transport and focusing. The multi-iodular configuration reduces risk by not scaling gnificantly beyond existing machines and offers the exibility of staged construction. It permits modular river testing at the full LMF operating level.

Introduction

An artist's concept of how one version of the LMF iight develop is shown in Fig. 1. Three 15-m high levels ould contain the 24 accelerator modules (eight per level) a closely packed, symmetric arrangement. Also shown e the extended MITLs that converge on the central rget section that includes the extraction diodes and the hromatic lens transport and focusing system. The main ody of this paper addresses the conceptual design of the

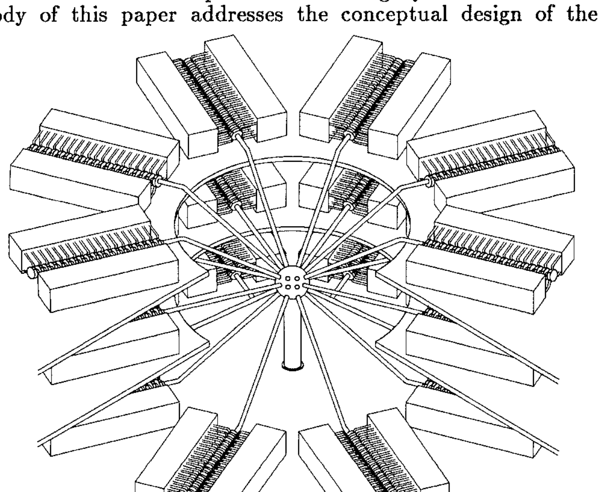

g. 1 Facility concept for the 24 module Sandia LMF.

celerator pulsed-power components. Marx generators, termediate Storage Capacitors (ISC), and Pulse Forming nes (PFL) that operate at >4 MV are within the esent technology. An inductive cavity design that ovides a 2.0 to 2.5-MV, ~1-MA, ~80-ns pulse to the ITL/Adder appears to be a reasonable extension of cent Sandia accelerators such as HERMES-III.[3] In dition to some design and modeling details, our scussion includes ramped pulses that support ion nching, vacuum stack inductance and cavity diameter nsiderations, and trade-offs between fewer higher stressed mponents and many lower stressed components.

Accelerator Modules

The fusion target design, established by numerical calculations and the existing ICF database, defines the ion diode operating parameters after the diode efficiencies and transport losses are accounted for. The diode parameters identify the minimum power requirements around which the MITLs and, in turn, the pulsed power accelerators that drive them, are designed. The general shape of the ion beam power pulse required to ignite an internal pulse shaping target design is shown in Fig. 2, along with the indicated ion kinetic energy. To produce such a waveform, we chose to add the outputs of two separate accelerator modules. In our design twelve "A" modules will produce a flat 65-TW, 50-ns pulse, and twelve "B" modules will generate the 650-TW, 20-ns pulse.

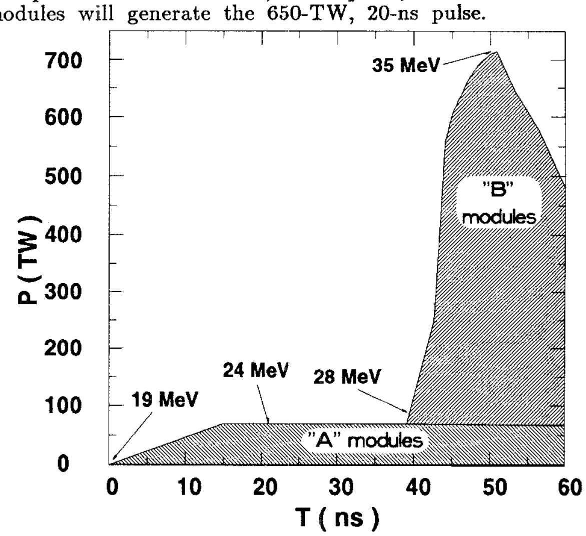

Fig. 2 Ion power pulse shape required to ignite target.

A-Modules: The lower power modules are based on components identical to those of HERMES-III. Each of 24 HERMES-III cavities will be driven by two 5-Ω, 1.1-MV, 60-ns PFLs. The matched load current is 440 kA. The present HERMES-III accelerator consists of 20 cavities, each driven by four PFLs (about 20% lower total voltage, but twice the current). Because that machine has been thoroughly discussed elsewhere, this paper will be concerned with the B-modules and focus on new aspects of our designs.

B-Modules: The B-modules meet the higher power requirements, while remaining comparable in size to the A-modules, by scaling up both the voltage and current in the new components. Seventeen cavities in this accelerator will each be powered by four 8-Ω, 2.25-MV (average), 80-ns PFLs that supply up to 1.3 MA peak current to a matched load. (It would take approximately 40 HERMES-III cavities to provide the same power.) Figure 3 is a layout of the B-module. According to our conceptual design, the overall module dimensions are about 24 m wide, 32 m long, and 5 m high. The total transformer oil volume for each B-module is approximately 1800 m^3. The pulse shaping section between the Marx generators and the cavities delivers a power gain of 19 with an energy transfer efficiency above 50%. The new hardware includes triaxial ISCs for efficient, compact, high voltage pulse shaping and stepped impedance PFLs to provide the desired voltage ramp for taking advantage of ion bunching.

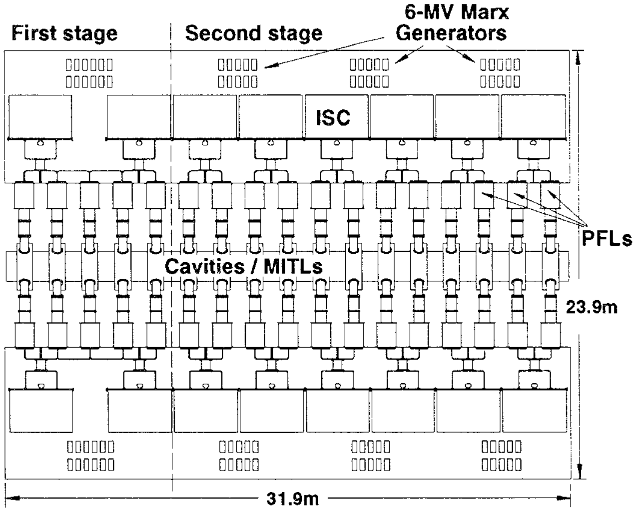

Fig. 3 The B-module accelerator as presently conceived.

MITL/Adder, Diode, and Transport Sections

Each module has two voltage adders and concentric extended MITLs to separately drive the two stages of the ion diode as indicated in Fig. 4.[1] The vertical dashed line in Fig. 3 indicates which portions of the accelerator drives each of the two stages. The MITL operating impedances for the A-modules and B-modules are 2.5 and 2.0 Ω, respectively. The MITLs will be undermatched at the diode to boost the load current and compensate for sheath current losses. The leading edge of the pulse is expected to suffer about 10 ns of erosion due to propagation in the long MITLs. Table I lists the total electrical parameters delivered to the diodes by all of the twelve A and twelve B modules, respectively.

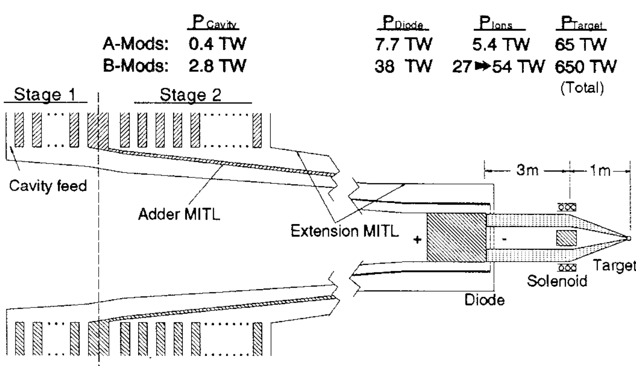

Fig. 4 The MITL/Adder, diode, and transport system.

TABLE I. Diode Pulsed Power Parameters

	A-Mods	B-Mods	Units
Power:	91	460	TW
1st Gap Voltage:	10	10	MV
2nd Gap Voltage:	15	26	MV
Current:	3.7	13	MA
Pulse Width:	60	40	ns
Energy:	5.5	10	MJ

Our present choice for an LMF light-ion source is the 2-stage extraction diode.[2] This diode offers improved control over the beam energy and current for either bunching or monoenergetic beams. The 2-Stage LMF diode parameters are designed to keep enhancement and divergence low, offering a potential divergence reduction to 6 mrad. A flat voltage profile at about 10 MV will dri the first stage 1-cm gap of the LMF diode. A current ramping from 0.8 to 1.1 MA in this gap, due to an assumed impedance drop, will be injected into the second accelerating gap. To accomplish the desired bunching in the B-modules, the injected current will be driven by a second stage accelerating voltage pulse with a 40-ns ramp The pulse from the second stage MITL/Adders varies fro about 16 to 26 MV. The beam inner and outer radii a 8 and 12 cm, respectively, at the 2-cm gap. The ion beam leaving each diode will have about a 32% voltage ramp and 38 TW peak power.

Figure 4 shows how the pulsed power accelerator, diode, and ion transport parameters are defined by the target requirements, assuming a 70% power efficiency fro the diode to the target.[1] The 20-ns long main power pulse will arrive at the 1.0-cm radius target with a 0.6-c FWHM Gaussian beam. The baseline transport scheme for LMF is a 4-m achromatic magnetic lens system with the geometry of Fig. 4.[4] The ion bunching occurs throughout the entire transport distance. With the diode solenoid-target achromatic system, focusing is not a function of voltage. The on-axis barricades shield the diodes from line-of-sight debris and radiation damage. T typical system would have a solenoid parameter ($B_z L$) of 82 T-cm and function with 1 Torr of helium.

Modeling and Design Techniques

We used the SCREAMER[5] circuit simulation code the majority of our initial analysis, because this code is convenient, fast, and inexpensive. It gives reliable result when all the destributed parameters that contribute some effect are included in the circuit model. The code topography allows a single main branch plus end branch which cannot form closed loops. Within this limit we modeled one full line from the Marx generator through t inductive cavity to the gaps that drive the MITL/Adder. The block diagram of the SCREAMER circuit model for the LMF B-module in Fig. 5 shows how all the addition parallel PFLs are lumped together and treated as end branches to achieve a realistic waveform propagating through the cavity. SCREAMER generates output pulse tables that can be incorporated as inputs to drive completely independent models starting at that point, th giving a consistent electrical model of the complete accelerator including the MITL/Adders and diode loads. A more general and flexible network simulation, SUPER-SCEPTRE,[6] was used to confirm some details that had be simplified with the SCREAMER circuit, such as the saturation and current loss properties of the cavity isolation cores. The JASON[7] electrostatic solver progran was a valuable tool for balancing the high stress electric fields and measuring region capacitances during the desig of the inductive cavities and the ISCs.

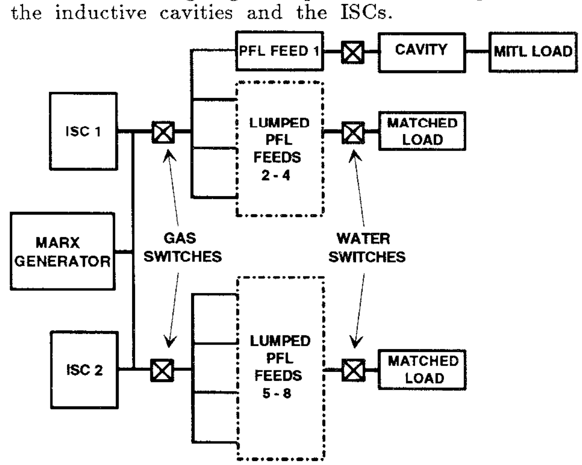

Fig. 5 Block diagram for LMF B-module circuit model.

Marx Generators

The primary energy storage/sources for each of the MF B-modules as indicated in Fig. 3 are the eight oil-ısulated Marx generators, very similar to those developed ›r the Particle Beam Fusion Accelerator (PBFA-II).[8,9] ix of them are composed of 60 (five rows), 3 μF, 100 kV ɪpacitors. These six each power eight PFLs via two ;Cs. They will produce about 745 kJ at 5.5 MV when ipolarly charged to 91 kV, and will drive the second ;age MITL/Adder. The remaining two Marx generators ill have an additional row of capacitors since they must ıch power ten PFLs to drive the first stage. They will roduce about 975 kJ at 6.8 MV when charged to 95 kV.

Intermediate Storage Capacitors

One-half of the 6-MV, 22-nF, triaxial ISC is shown ı the right in Fig. 6. A pair of ISCs couple each Marx ›nerator to eight PFLs (ten for the first stage). As an termediate pulse shaping stage, the ISC shortens the FL charging time and improves the energy transfer ficiency. With the middle cylinder charged to high ltage, we take advantage of the inner and outer ionized water volumes and reduce the outside dimension a more manageable size than the conventional coaxial ıter capacitor would allow at these field stresses. For rposes of analysis it can be treated as nested coaxial es in parallel. The inner/outer radii for the inside and tside lines are 28.2/109 cm and 110/175 cm, ;pectively, giving an effective impedance of 2.3 Ω. The erall length of this water bottle is 2.5 m. From timistic breakdown formulas, the largest ratio of average ctric field stress to the calculated breakdown stress /F) is 0.8 at the outside of the charged conductor. e peak field stresses on the 4-in thick polyurethane /water barrier are kept below 100 kV/cm with an ɜrage of 80 kV/cm. With a charging time of 1.35 μs, ISCs for the first and second stages reach 312 kJ at MV and 260 kJ at 5.1 MV, respectively.

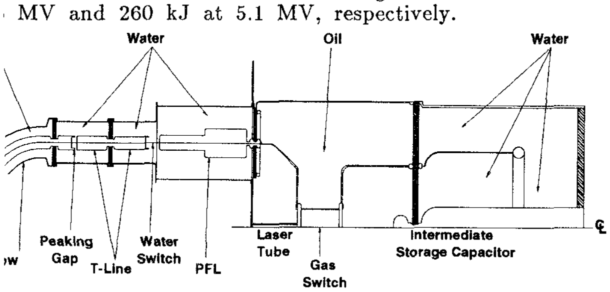

. 6 Pulse shaping section for the LMF B-module.

Laser Triggered Gas Switches

Our switch of choice for discharging the ISCs is the FA-II Rimfire switch[10] which is presently operating near LMF switching parameters. Since the low-jitter, laser ;gered, SF_6-filled switch will require only minor difications to increase its stand-off voltage by ~10% and peak transfer current by ~25% (to 640 kA), no ıificant design effort has yet been spent on the new tch. Our circuit simulations modeled the Rimfire tch as a 400-nH inductor in series with an onentially increasing resistance using an e-folding time stant of 2.6 ns. It closes at about 89% of the ringover ;age peak.

Pulse Forming and Transmission Lines

Because the first gap of the 2-stage diode will require ɜlatively flat voltage pulse shape to drive it, and the ›nd gap needs a specified voltage ramp, two PFL metries are necessary. The first stage PFL will be a ight 8-Ω coaxial line with a deionized, deaerated water ectric. After trying a variety of shapes for the inner conductor in our circuit models, we have selected our second stage PFL to have a "stepped" geometry as indicated in Fig. 6. This novel dual impedance PFL is easy to make, as well as to model. While the average impedance is still 8 Ω, the slope of the final ramp is sensitive to the spread of the first and second PFL impedances around the average. For our particular circuit model parameters, a 7-Ω to 9-Ω step results in a 40-ns ramped output with a $\Delta V/V_{avg}$ of about 34%, while a larger 6-Ω to 10-Ω step produces a ~41% ramp.

The PFLs of the B-modules have a 40-ns one-way transit time. They are switched at about 4.6 MV by self-breaking multi-channel water switches that must transfer up to 350 kA. Like the gas switch model, the ~12-cm gap, 3-channel water switch is modeled as an exponentially decreasing resistance, with an e-folding time of 5.0 ns, in series with a 78-nH inductance. If we later determine that the water switch losses, inductance, or jitter will be excessive, it is possible to add another coaxial water line in series after the first water switch to use the double-bounce charging technique[11] which allows smaller gap spacings and earlier closure before peak charging voltage.

The 80-ns PFL output pulse travels along a 40-ns long, 8-Ω coaxial water line, a water peaking gap and pre-pulse shield, and then a 45° elbow that feeds the cavity. The peaking water switch is modeled as a 2-cm gap, with five current carrying channels, 11-nH inductance, and a 1.3-ns e-folding time. It closes within the first half of the output pulse risetime.

Inductively Isolated Cavities

A cross section of the 2.5-MV, 23-nH inductive cavity showing the Vacuum Insulator Stack (VIS) and the inductive isolation cores is seen in Fig. 7. The cavity inner bore that forms the outer surface of the MITL is 1.52 m, and the axial length is about 0.97 m. An MITL matched to the average output voltage (~2-Ω operating impedance, ~3-Ω vacuum impedance) would have a gap spacing of about 3.6 cm at the first cavity. We designed the cavity for field stresses as high as our calculations would reasonably allow and for a relatively low inductance. A good figure of merit of 10 nH/1 MV seems achievable. Too much inductance causes a voltage overshoot and excessive stress at the insulator stack and a corresponding amplitude loss with risetime degradation at the cavity output. The bore size is typically driven up by the low inductance requirement and by the mechanical aspect ratio for supporting the concentric MITLs. It is driven down by overall hardware size and cost. Circuit simulations using our B-module cavity parameters generate the desired ramped output waveforms as defined by the PFL shape. Examples of cavity output voltage and power pulse shapes for a 6-Ω to 10-Ω PFL model are seen in Fig. 8.

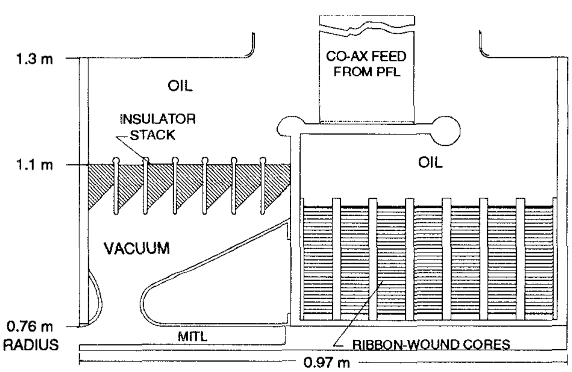

Fig. 7 The 2.5-MV inductive cavity cross-section.

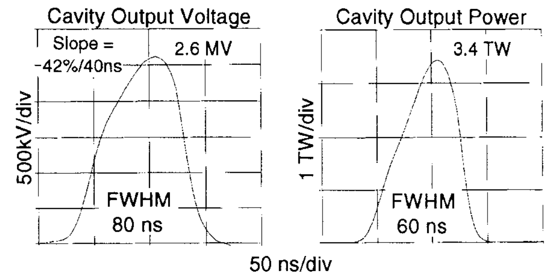

Fig. 8 Simulated cavity output voltage and power.

Ferromagnetic Cores

As indicated in Fig. 7, seven toroidal cores of 5.08-cm ribbon-wound amorphous metal alloy, such as the type 2605 CO Metglas by Allied Corp. or the Vitrovac 7600 Z by Vacuumschmelze, are sufficient to provide the 0.18 Volt-sec inductive isolation between neighboring cavities. Our design assumes a 3.3-T ΔB-swing and 0.7 core packing factor. The number of the cores and the thickness of the insulators separating them are determined by the electric fields. We kept the average field stress along the vertical faces of these cores below 15 kV/cm. The core inner and outer diameters are about 79 cm and 100 cm, respectively. In the SUPER-SCEPTRE circuit model we simulate the core loss/saturation effect by treating the magnetic cores as time-varying, nonlinear resistors in series with a fixed inductor that represents the saturated core inductance; these act as current shunts across the output load. The effective nonlinear resistance is a mixed function of geometry, material properties, and circuit parameters.

Vacuum Insulator Stacks

Seven 5.08-cm thick Lucite insulator rings and six 0.74-cm thick aluminum grading rings form the VIS, as shown in Fig. 7. Since the diodes and target section are far removed from the VISs, the insulators should not suffer degradation from ultraviolet or x-radiation. The length of the stack was chosen so the average electric field stress would be 70 kV/cm for a 2.5-MV applied voltage. Accounting for the pulse length and multiple-cavity large area effects, we estimate the average stress to breakdown field ratio to be 0.82. Longer stacks would appear to improve this safety margin, but they also increase the cavity inductance and thus the voltage overshoot which begins to negate the improvement.

Another trade-off in the VIS design is field grading uniformity versus cost. Using more, thinner rings will result in a more uniformly graded field across the total length of the VIS. From our initial design efforts, an eight-insulator stack will see +14%/-8% excursions about the average compared to +18%/-11% with seven insulators for the same total insulator length, while holding the cavity geometry fixed. The cost of large hardware items such as these rings, cavity housings, or polyurethane barriers is driven primarily by the quantity and the largest dimension. A seven-insulator stack for all the LMF B-modules could save as much as $1.8 M over the eight-insulator stack, for example! We expect further design effort on the cavity conductor shapes to improve the grading on the seven-insulator stack and make it even more attractive. Resources versus risk considerations are having an increasing impact on large scale system designs.

Concluding Remarks

The Sandia LMF design, which satisfies the target power and energy requirements to achieve ignition and gain, is based on the successful accelerator technology use in HERMES-III and the recent results from the PBFA-II light ion fusion program. Our configuration offers the flexibility of staged construction plus reduced risk. This concept permits modular development and independent driver testing at the full LMF operating levels. The 2-stage diode promises improved efficiency, beam control, and reduced divergence. The achromatic lens system focuses the ions even as the voltage changes, minimizes debris, and shields the diode.

The overall driver energy transfer efficiency will be between 15 and 23% depending on how some design issu are resolved. There will be an efficiency-cost trade-off fo ion bunching and focusing. The positive polarity MITL may be less efficient than the negative polarity configuration. Also, there may be time-dependent divergence losses at the target. The final LMF design w evolve as we continue to apply creative component development and learn from component performance on t PBFA-II, HERMES-III, Sabre, and Cornell University machines, among others.

Acknowledgements

This work was supported by the U.S. Department (Energy under contract DE-AC04-76DP00789. Our appreciation is extended to Don Cook for his encouragement and guidance. For providing us with son of the figures that clearly express our concepts, we thank Gary Douglas of Rockwell Power Systems. Special thank go to the Ignition Concepts Review Panel that met on May 14-15, 1992 and, upon a detailed briefing, responded with their findings and recommendations. Panel member include John Greenly of Cornell University; Tom Hussey Phillips Lab; Ian Smith and Phil Spence of Pulse Science Inc.; and Cliff Mendel, Ken Prestwich, Jim Rice, and Ju Ramirez (Chairman) of Sandia Labs.

References

[1] M. G. Mazarakis, et. al. "The LMF Triaxial MITL Voltage Adder System," Paper 10-4 This Conference.

[2] T. R. Lockner, et. al. "Theoretical and Experimental Studies of the 2-Stage Diode," Paper 13-1 This Conference.

[3] J. J. Ramirez, et. al. "The HERMES-III Program," Proc. 6th IEEE Pulsed Power Conf., Arlington, VA, June 29-July 1, 1987.

[4] C. L. Olson, "Achromatic Magnetic Lens Systems for High Current Ion Beams," Proc. 1988 Linear Accelerator Conf., CEBAF Report 89-001, Williamsburg, VA, Oct 3-7, 1989.

[5] M. M. Widner and M. L. Kiefer, "SCREAMER - A Pulsed Power Design Tool, User's Guide," Sandia Nat. Labs, Albuquerque, NM, Apr 25, 1985.

[6] J. C. Bowers and S. R. Sedore, "SCEPTRE: A Computer Program for Circuit and System Analysis," Englewood Cliffs, NJ, Prentice Hall, 1971.

[7] S. J. Sackett, "JASON - A Code for Solving General Electrostatics Problems, User's Manual," CID-17814, Lawrence Livermore Nat. Labs, Livermore, CA, 1978.

[8] L. X. Schneider, "Development of a High Reliability 6.0 MV, 390 kJ Marx Generator," Proc. 4th IEEE Pulsed Power Conf., Albuquerque, NM, June, 1983.

[9] J. M. Wilson, "PBFA-II Energy Storage Section Design," Proc. 4th IEEE Pulsed Power Conf., Albuquerque, NM, June, 1983.

[10] D. R. Humphreys, et. al. "Rimfire: A Six Megavolt Laser-Triggered Gas-Filled Switch for PBFA-II," Proc. 5th IEEE Pulsed Power Conf., Arlington, VA, June 10-12, 1985.

[11] I. Smith, "Rapid Charging of Transmission Lines," Pulse Sciences, Inc, Oakland, CA, Interim Report, Sandia Nat. Labs, Apr, 1981.